Letter to the Editor

Human plasma C3 is essential for the development of memory B, but not T, lymphocytes

To the Editor:

Primary C3 deficiency is an extremely rare autosomal-recessive disease, with fewer than 50 families described worldwide. Plasma and intracellular C3 are considered B-cell receptor (BCR) and T-cell receptor (TCR) costimulators, respectively, but their contribution to lymphocyte biology remains obscure, particularly in humans. Reduced plasma C3 can be caused not only by primary C3 deficiency, due to loss-of-function *C3* mutations, but also by secondary C3 deficiency or C3 consumption, due to gain-of-function *C3* mutations or due to mutations in C3 regulators such as complement Factor I *(CFI)*.[1] We reasoned that comparing B- and T-cell differentiation and function in primary and secondary plasma C3 deficiency might help to understand the role of plasma and intracellular C3 in adaptive immunity. We report the immunological features of lymphocytes from 9 individuals with low plasma C3 belonging to 6 families, with mutations causing primary or secondary C3 deficiency and, in some cases, chronic kidney disease stages 1 to 3 (see Fig E1, *A*, and Tables E1 and E3 in this article's Online Repository at www.jacionline.org).

To study whether reduced plasma C3 levels could affect lymphocyte differentiation, patients, healthy carriers (HCs), and healthy donors (HDs) were immunophenotyped and compared for several T- and B-cell subsets, including those representing successive differentiation and effector subsets. Absolute lymphocyte numbers were always within normal ranges (not shown). T-lymphocyte differentiation was essentially normal, and no significant differences, except for increased follicular helper T-cell frequency, were detected when individuals above (HCs + HDs) or below (patients) 40 mg/dL plasma C3 (Fig E1, *B*) were compared (see Fig E2 in this article's Online Repository at www.jacionline.org). In contrast, impaired naive to memory B-cell differentiation was observed in both primary and secondary plasma C3–deficient patients (Fig 1, *A*), with increased naive ($CD19^+IgD^+CD27^-$) B cells, and reduced unswitched ($CD19^+IgD^+CD27^+$) and switched ($CD19^+IgD^-CD27^+$) memory B cells. Such changes were statistically significant when plasma C3 levels were below the 40 mg/dL threshold (Fig 1, *B*).

B-cell regulation by complement involves antigen opsonization by C3d and recognition through CD21/CR2, a component of the B-cell coreceptor,[2] which lowers the threshold for B-cell activation.[3] To determine a possible role of circulating C3-opsonizing fragments in the generation of memory B cells, we analyzed the correlation between plasma C3 levels and B- or T-cell

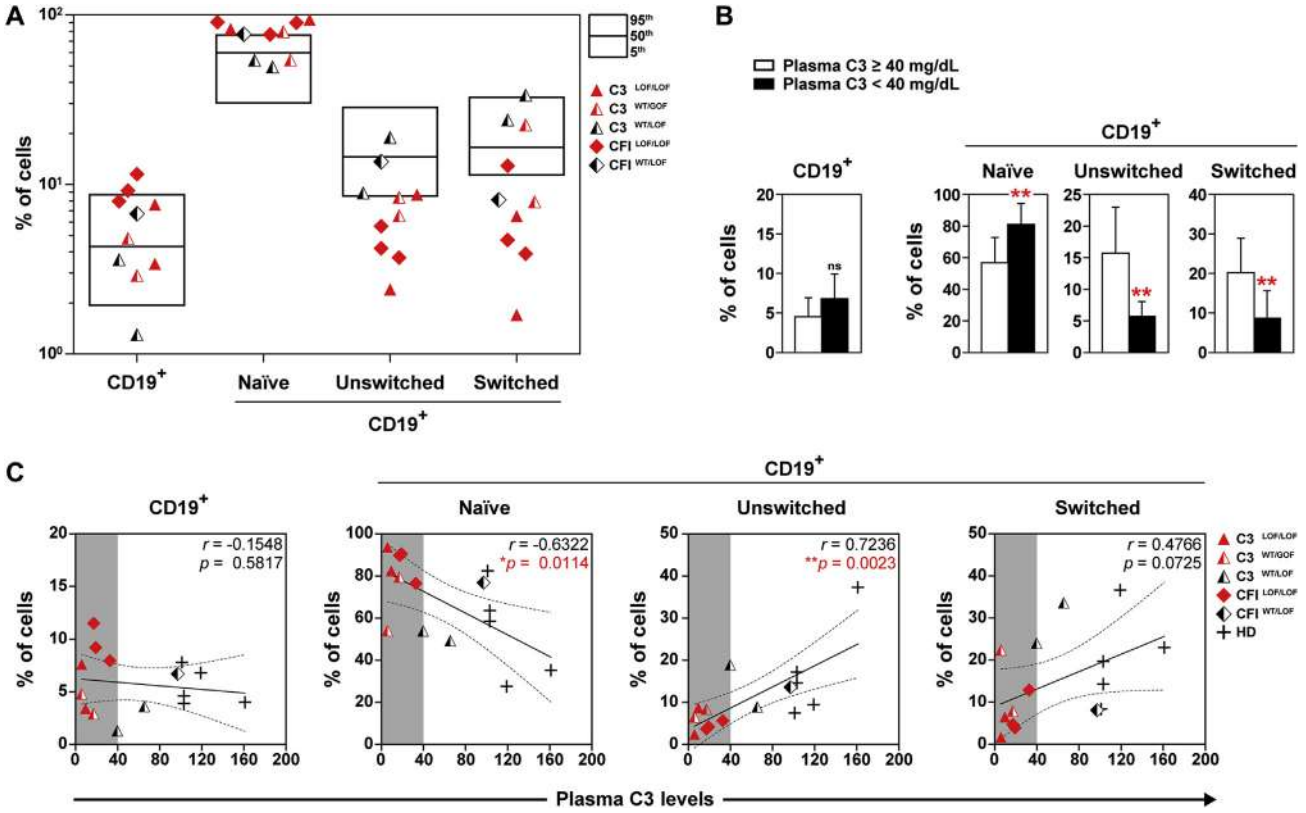

FIG 1. B-lymphocyte immunophenotype. **A,** B-cell subset frequencies compared with normal percentiles (n = 10 HCs + patients vs 12 HDs). Symbols as in Fig E1, *B*. **B,** B-cell subsets (mean + SD) of individuals below (patients) or above (HDs + HCs) the 40 mg/dL plasma C3 threshold (gray area in *C*). **C,** Correlation analysis (Pearson *r*) of B-cell subsets and plasma C3 levels. *HC,* Healthy carrier; *HD,* healthy donors; *ns,* nonsignificant. Solid lines are best-fit linear regressions; dashed lines are 95% CIs. $*P < .05$ and $**P < .01$.

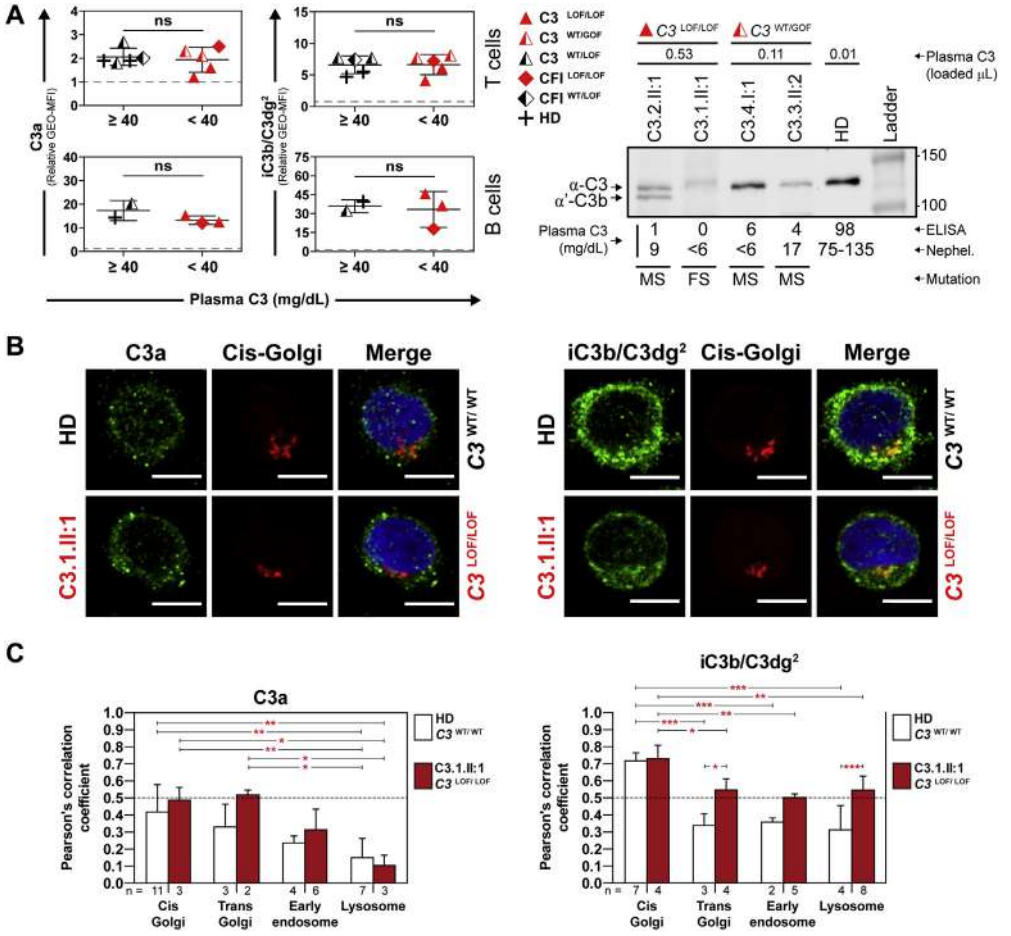

FIG 2. C3 detection in T-cell lines and plasma from C3-deficient patients. **A,** *Left,* Intracellular C3 fragments in single cell lines from donors above or below the 40 mg/dL plasma C3 threshold (flow cytometry). Data are mean ± SD of GEO-MFI relative to isotype controls (dashed lines). *ns,* Nonsignificant. *Right,* Extracellular C3 detection by Western blot (α chain) vs ELISA and nephelometry (mg/dL means or range) in plasma from primary (MS, missense and FS, frameshift) and secondary (MS) C3-deficient patients. **B,** Subcellular T-cell colocalization of C3 fragments with cis-Golgi (confocal microscopy ×60 using 1 C3a- and 2 iC3b/C3dg-specific mAb, scale bars 5 µm). **C,** Statistical analysis of C3 fragment colocalization with several subcellular compartments (mean + SD; only $r > 0.5$ [dashed horizontal lines] were considered; $P <$ *.05, **.01, ***.001).

subpopulations in our cohort. The results showed a statistically significant positive correlation of plasma C3 levels with the frequency of unswitched memory B cells, and negative correlation with that of naive B cells, but not with total B cells (Fig 1, *C*). A nonsignificant positive correlation was also found with switched memory B-cell levels. In contrast, none of the T-cell subpopulations analyzed correlated with plasma C3 levels (see Fig E2, *C*). Although impaired memory B-cell differentiation has been reported in a gain-of-function plasma C3–deficient patient,[4] here we demonstrate in a larger cohort that reduced plasma C3 levels, whether primary or secondary, result in a selective defect in the *in vivo* differentiation of memory B, but not T, lymphocytes.

To explore whether the defect in memory B-cell development caused by C3 deficiency was associated with altered T- or B-cell function, PBMCs were studied. *Ex vivo* T- and B-cell function, measured as proliferation in response to mitogens (see Fig E3 in this article's Online Repository at www.jacionline.org), or *in vivo* B-cell function, measured as immunoglobulin or vaccine-specific antibody levels (see Table E2 in this article's Online Repository at www.jacionline.org), was mostly normal in our cohort, despite their low plasma C3 levels. Although C3 deficiency has been associated with recurrent bacterial infections[1] and decreased proliferation against specific recall antigens, neither primary nor secondary plasma C3–deficient patients in our cohort (or other's[5]) showed clinical features suggestive of severe T- or B-cell defects. However, our findings may be clinically relevant to improve patient management in countries where health conditions or vaccinations are below Western standards.

Both B and T lymphocytes contain intracellular C3 fragments.[6] Indeed, it was shown that cathepsin-L–cleaved intracellular C3 was required for T-cell homeostasis and, upon TCR engagement, increased and participated in T_H1 responses. Hence, we generated pure T- and B-cell lines from our cohort and analyzed their intracellular C3 content by flow cytometry using specific mAb against 2 C3-associated neoepitopes (see Fig E4 in this article's Online Repository at www.jacionline.org). The results showed that all tested cell lines derived from primary or secondary plasma C3–deficient patients, above or below 40 mg/dL plasma C3, expressed intracellular C3 fragments at HD levels

(see Fig 2, *A*, left; see Fig E5, *A*, in this article's Online Repository at www.jacionline.org). In addition, intracellular C3a was increased after TCR activation of C3-deficient T-cell lines (see Fig E5, *B*). These observations are in line with previously unexpected published data[6] and prompted a closer analysis of plasma C3 levels by Western blot and ELISA (Fig 2, *A*, right). The results showed that even primary, and expectedly secondary, C3-deficient plasmas have very low levels of C3 proteins, which may thus accumulate in cellular compartments and allow intracellular detection. Of note, the presence of iC3b/C3dg fragments in cells from factor I (fI)-deficient patients suggested fI-independent cleavage in lymphocytes.

Intracellular localization studies revealed that C3a and iC3b/C3dg fragments showed different subcellular locations, with iC3b/C3dg, but not C3a (which has previously been shown to be located in the lysosomes in T cells[6]), found predominantly associated with the cis-Golgi (Fig 2, *B* and *C*). These results suggest a differential intracellular location of the cleaving enzymes generating these complement fragments.[7] Interestingly, T-cell lines from primary plasma C3 deficiency showed accumulation of all C3 tested fragments in several subcellular compartments, particularly in lysosomes, which may impair exocytosis of C3 (Fig 2, *C*, right).

Taken together, these results indicate that although intracellular C3 expression in lymphocytes occurs despite severe plasma C3 deficiency, it cannot replace plasma C3 for memory B-cell differentiation. The present data support our previous suggestion that human C3 deficiency is always leaky to some extent and that complete combined intracellular and extracellular C3 (or C5) deficiency may not be viable in humans.[8] A mechanism bridging innate and adaptive immunity thus emerges connecting B-cell coreceptor recognition of C3 fragments, in a concentration-dependent manner, and memory B-cell differentiation. We hypothesize that reduced plasma C3 impairs the generation of C3-activating/opsonizing fragments such as C3dg/C3d. In turn, BCR coactivation through CD21/CR2 would be impaired, hampering sufficient signaling for the generation of memory B cells. Note that this would not affect the generation of antigen-specific antibodies later on (see Fig E6 in this article's Online Repository at www.jacionline.org). See this article's Discussion section in this article's Online Repository.

In summary, despite the small size of the cohort, we report a side-by-side study of B- and T-cell features in the very rare conditions of C3 and fI deficiencies. Our results show that plasma C3 is essential for the development of memory B, but not T, lymphocytes in a plasma C3 level–dependent fashion, and demonstrate that very low plasma C3 levels do not preclude the expression of intracellular C3 fragments in lymphocytes.

We thank all patients, families, HDs, clinicians, and researchers for their cooperation, particularly M. S. Mazariegos, P. Roda-Navarro, R. Ramirez-Munoz, P. Castro-Sánchez, M. Pérez-Andrés, and J. A. Camacho-Diaz, members of Secugen S.L. and the DNA sequencing laboratory at CIB for their help with patient sequencing and genotyping, and Mercedes Domínguez for the anti-iC3b/C3dg neoepitope antibodies.

Anaïs Jiménez-Reinoso, PhD[a]
Ana V. Marin, MSc[a]
Marta Subias, PhD[b,c]
Alberto López-Lera, PhD[c,d]
Elena Román-Ortiz, MD[e]
Kathryn Payne, BSc Hons[f]
Cindy S. Ma, PhD[f,g]
Giuseppina Arbore, PhD[h]
Martin Kolev, PhD[h]
Simon J. Freeley, PhD[h]
Claudia Kemper, PhD[h]
Stuart G. Tangye, PhD[f,g]
Edgar Fernández-Malavé, PhD[a]
Santiago Rodríguez de Córdoba, PhD[b,c]
Margarita López-Trascasa, PhD[c,d]
José R. Regueiro, PhD[a]

From [a]the Department of Immunology, Complutense University School of Medicine and 12 de Octubre Health Research Institute (imas12), Madrid, Spain; [b]the Centro de Investigaciones Biológicas (CSIC), [c]the Centro de Investigación Biomédica en Red de Enfermedades Raras (CIBERER), and [d]the Immunology Unit, Hospital Universitario La Paz, IdiPAZ, Madrid, Spain; [e]the Servicio de Nefrología Pediátrica, Hospital La Fe, Valencia, Spain; [f]the Immunology Research Program, Garvan Institute of Medical Research, Darlinghurst, Australia; [g]the St Vincent's Clinical School, University of New South Wales, Sydney, Australia; and [h]the MRC Centre for Transplantation, Division of Transplant Immunology and Mucosal Biology, King's, College London, London, United Kingdom. E-mail: regueiro@med.ucm.es.

This study was supported by Ministerio de Economia y Competitividad (MINECO) (grant nos. SAF2011-24235 and SAF2014-54708-R to J.R.R., grant nos. SAF2011-26583 and SAF2015-66287-R to S.R.dC., and grant no. PI15-00255 to M.L.T.), by Comunidad de Madrid (grant nos. S2010/BMD-2316 and B2017/BMD-3673 to J.R.R., S.R.dC., and M.L.-T.), by Fundación Lair (grant no. 2012/0070 to J.R.R.), by Ciber de Enfermedades Raras (CIBERER to S.R.dC. and M.L.-T.), and by the Seventh Framework Programme European Union Project EURenOmics (grant no. 305608 to S.R.dC.). S.R.dC. is a member of the CIB Intramural Program "Molecular Machines for Better Life" (MACBET). A.J.-R. was supported by MINECO (grant no. FPI BES-2012-055054) and EFIS-IL (EFIS-IL Short-Term Fellowship), A.V.M. by Comunidad de Madrid (grant no. S2010/BMD-2316) and Universidad Complutense (grant no. CT46/15), and A.L.-L. by MINECO and CIBERER. Work in the Kemper Laboratory was supported by the MRC Centre (grant no. MR/J006742/1), a European Union–funded Innovative Medicines Initiative BTCURE (C.K.), a Wellcome Trust Investigator Award (C.K.), the National Institute for Health Research Biomedical Research Centre based at Guy's and St Thomas' National Health Service Foundation Trust and King's College London, and the King's Bioscience Institute at King's College London (G.A.). S.G.T. and C.S.M. are supported by grants and fellowships from the National Health and Medical Research Council of Australia (grant nos. 1113904 and 1042925), and the Office of Health and Medical Research of the New South Wales State Government.

Disclosure of potential conflict of interest: The authors declare that they have no relevant conflicts of interest.

REFERENCES

1. Reis ES, Falcão DA, Isaac L. Clinical aspects and molecular basis of primary deficiencies of complement component C3 and its regulatory proteins factor I and factor H. Scand J Immunol 2006;63:155-68.
2. Matsumoto AK, Martin DR, Carter RH, Klickstein LB, Ahearn JM, Fearon DT. Functional dissection of the CD21/CD19/TAPA-1/Leu-13 complex of B lymphocytes. J Exp Med 1993;178:1407-17.
3. Dempsey PW, Allison ME, Akkaraju S, Goodnow CC, Fearon DT. C3d of complement as a molecular adjuvant: bridging innate and acquired immunity. Science 1996;271:348-50.
4. Ghannam A, Pernollet M, Fauquert JL, Monnier N, Ponard D, Villiers MB, et al. Human C3 deficiency associated with impairments in dendritic cell differentiation, memory B cells, and regulatory T cells. J Immunol 2008;181:5158-66.
5. Okura Y, Kobayashi I, Yamada M, Sasaki S, Yamada Y, Kamioka I, et al. Clinical characteristics and genotype-phenotype correlations in C3 deficiency. J Allergy Clin Immunol 2016;137:640-4.e1.
6. Liszewski MK, Kolev M, Le Friec G, Leung M, Bertram PG, Fara AF, et al. Intracellular complement activation sustains T cell homeostasis and mediates effector differentiation. Immunity 2013;39:1143-57.
7. Théry C, Ostrowski M, Segura E. Membrane vesicles as conveyors of immune responses. Nat Rev Immunol 2009;9:581-93.
8. Hess C, Kemper C. Complement-mediated regulation of metabolism and basic cellular processes. Immunity 2016;45:240-54.

https://doi.org/10.1016/j.jaci.2017.09.037

METHODS

Donors, complement profile, genetic diagnosis, and lymphocyte isolation

Ten different individuals (9 with low plasma C3 levels, 7 below 40 mg/dL and medium/long-term clinically diagnosed disease, see Table E3) belonging to 6 different families with primary (due to loss-of-function, LOF, *C3* mutations) or secondary (due to gain-of-function, GOF, *C3* mutations, or due to LOF complement Factor I or *CFI* mutations) plasma C3 deficiency were studied (Fig E1). In all cases, age- and sex-matched HDs were included ($n \leq 18$). Plasma C3 levels and genetic data are summarized in Table E1. Healthy carriers (HCs) and patients were classified according to their primary or secondary C3 deficiency, their LOF/GOF mutated or wild-type (WT) alleles for *C3* or *CFI* (WT/LOF; LOF/LOF; WT/GOF), but also by an arbitrary 40 mg/dL threshold for very low plasma C3 levels observed in all patients with clinical features (Fig E1, *B*). All HCs and HDs had plasma C3 level of greater than or equal to 40 mg/dL. In figure legends, full red and red/white symbols denote homozygous or heterozygous individuals, respectively, with plasma C3 level of less than 40 mg/dL and clinical features. Black/white symbols identify HCs. Triangles and rhombuses identify individuals with mutations in *C3* or *CFI,* respectively.

C3 and *CFI* mutations screening and genotyping were performed as described.[E1,E2] Plasma C3 levels were measured by nephelometry or ELISA. PBMCs were isolated from peripheral blood (EDTA) by density-gradient centrifugation (Ficoll Paque Plus, GE Healthcare, Little Chalfont, United Kingdom).

All samples were obtained after written informed consent from the donors or their guardians, and all studies were performed according to the principles expressed in the Declaration of Helsinki and approved by the Institutional Research Ethics Committees of the hospitals involved.

Case reports (see Table E3 for further details)

C3.1.II:1 is an 18-year-old membranoproliferative glomerulonephritis (MPGN) type I primary plasma C3–deficient patient of Pakistani origin diagnosed at age 9 years, born to consanguineous parents. From age 12 to 15 years he suffered from IgA-negative cutaneous episodes of vasculitis and knee arthralgia resembling Henoch-Schönlein purpura (HSP). He also suffered 1 severe episode of pneumonia with pleural effusion that required draining. Despite signs of microhematuria and microalbuminuria, renal function was preserved. Renal biopsies showed C3-negative linear glomerular deposits with intense immunofluorescence staining (4/4) for IgM, C4 and C1q and intermediate (3/4) for IgA, IgG, kappa and lambda chains, as well as focal mesangial deposits weakly staining for IgA, IgG, C4, and C1q. C3.1.I:1 is his HC father with low plasma C3 levels.

C3.2.II:1 is a 13-year-old Spanish MPGN immunofluorescence-negative primary plasma C3-deficient patient diagnosed at age 1 year, who presented macroscopic hematuria and proteinuria in the nephritic range but no signs of renal dysfunction or infectious disease. As observed in C3.1.II:1, he presented recurrent HSP-like IgA-negative vasculitis in the lower limbs. He received a complete immunization with 2 doses of Prevenar before age 2 years and showed high pneumococcus-specific IgG titers after a dose of Pneumococcal polysaccharide vaccine (PPV-23, Pneumovax23) at age 8 years. He also displayed nonimmune hemolytic anemia associated with splenomegaly. Enzymatic disorder and paroxysmal nocturnal hemoglobinuria were ruled out. Immunofluorescence staining of renal biopsies was repeatedly negative. C3.2.I:2 is his HC mother with low plasma C3 levels.

C3.3.II:2 is a 40-year-old Spanish MPGN type I secondary plasma C3–deficient patient diagnosed at age 23 years. When he was 15 years old, he suffered a sepsis episode with generalized HSP and renal insufficiency, presently persistent reduced C3 levels in serum, proteinuria, and mild hematuria. A renal cortex biopsy showed a high proportion of sclerotized glomeruli. Nonsclerotized glomeruli showed a lobulated morphology and mesangial proliferation, endocapillar hypercellularity, and capillary wall thickening. Direct immunofluorescence revealed intense granular C3 staining in the mesangium and peripheral regions and weakly intense staining of IgM, C1q, kappa chains, and IgA in peripheral subendothelial regions.

C3.4.I:1 is a 49-year-old healthy secondary plasma C3–deficient Spanish man with mild proteinuria and microhematuria diagnosed at age 45 years.

CFI.1.II:1 is a 39-year-old woman with secondary plasma C3 deficiency due to a homozygous mutation in *CFI* reported previously.[E2,E3] She was diagnosed at 23 years, but she debuted at age 16 years with a meningococcal septicemia coincident with menstruation. From age 22 years, she developed up to 20 monthly recurrent episodes of acute meningitis around the perimenstrual period. Her younger sister aged 30 years (CFI.1.II:4) has the same genotype and secondary plasma C3 deficiency, and also suffered 1 meningitis episode.

CFI.2.II:2 is a 53-year-old woman with secondary plasma C3 deficiency due to a homozygous mutation in *CFI*[E2] diagnosed at age 19 years. She suffered several episodes of otitis during childhood and was diagnosed of juvenile chronic polyarthritis and HSP at age 11 years. She suffered meningococcal meningitis at age 17 years and meningococcal pneumonia at age 19 years. Two of her siblings have a clinical history of infectious diseases (otitis, septic arthritis, and lymphocytic meningitis). She is presently asymptomatic.

Extracellular flow cytometry

The following mAbs were used: CD3 (A07746), CD4 (A07751, A07752), CD8 (A07756, A07758), CD19 (A07771), and CD45RA (IM0584U) from Beckman Coulter (Brea, Calif); CD27 (555440), CD31 (555446), IgD (555779), and TCRγδ (333141) from BD Biosciences (San Jose, Calif); and TCRαβ (306717) from BioLegend (San Diego, Calif). FACSCalibur instrument (BD Biosciences) and CellQuestPro (BD Biosciences) and FlowJo (Tree Star, Ashland, Ore) software were used for the analysis.

Gating strategy for B immunophenotype: $CD19^+$ lymphocytes were analyzed for IgD^+CD27^- (naive), IgD^+CD27^+ (unswitched), and IgD^-CD27^+ (switched) cell distributions.

Gating strategy for T immunophenotype: Lymphocytes were analyzed for $CD3^+$, $\alpha\beta^+$, or $\gamma\delta^+$ cell distribution; $CD3^+$ lymphocytes were analyzed for $CD4^+$ and $CD8^+$. Gating strategy for $CD4^+$ T-cell subsets: $CD4^+CD45RA^+CD31^+$ (recent thymic emigrants), $CD4^+CD45RA^+CD31^-$ (central naive), $CD4^+CD25^{lo}CD127^{hi}CXCR5^-CD45RA^+$ (naive), $CD4^+CD25^{lo}CD127^{hi}CXCR5^-CD45RA^-$ (memory), $CD4^+CCR7^+CD45RA^-$ (central memory), $CD4^+CCR7^-CD45RA^-$ (effector memory), $CD4^+CD25^{hi}CD127^{lo}$ (regulatory T), and $CD4^+CD25^{lo}CD127^{hi}CXCR5^+$ $CD45RA^-$ (follicular helper T).[E4] T_H1 ($CXCR3^+CCR6^-$), T_H2 ($CXCR3^-CCR6^-$), T_H17 ($CXCR3^-CCR6^+$), and T_H1/T_H17 ($CXCR3^+CCR6^+$) subsets were analyzed within the subpopulation of memory $CD4^+$ T cells. Analysis and gating strategy for $CD8^+$ T-cell subsets was performed as previously described.[E4,E5]

Proliferation in response to mitogens and antibody titers

PBMCs were stained with carboxyfluorescein succinimidyl ester (from Molecular Probes, Eugene, Ore) and cultured in RPMI-1640 supplemented with 10% FBS for 5 days after stimulation with 1 μg/mL plate-coated anti-CD3 (UCHT-1, OKT3; eBioscience, Waltham, Mass), 5 μg/mL *Phaseolus vulgaris* leucoagglutinin (PHA), 10 ng/mL phorbol 12-myristate 13-acetate and 1 μM ionomycin, 8 μg/mL *Phytolacca americana* pokeweed mitogen (PWM) (Sigma-Aldrich, St Louis, Mo), or 10 ng/mL superantigens (*Staphylococcal* Enterotoxin B or E; Toxin Technology, Inc, Sarasota, Fla). Carboxyfluorescein succinimidyl ester dilution was analyzed by flow cytometry as reported.[E6] Vaccine-specific serum antibody titers were determined with ImmunoCAP Rc208 kit (for anti–tetanus toxoid IgG levels) (Phadia, Uppsala, Sweden), Human anti-Diphtheria Toxoid IgG EIA kit (Binding Site, Birmingham, UK), Rubella ELISA IgG kit (Vircell, Granada, Spain), Varicella ELISA IgG kit from Vircell, and Enzygnost anti-Measles virus IgG kit (Siemens, Marburg, Germany). Antipneumococcal IgG titers were measured with an in-house ELISA using Pneumo23polysaccharide pneumococcal vaccine as antigen and HRP-labeled goat antihuman IgG as detection antibody.

Generation of transformed T- and B-cell lines

Human T-cell lymphotropic virus type 1–transformed T-cell lines, which have been reported to synthesize higher intracellular C3 than resting or

activated primary T cells,[E7] were generated as reported,[E8] and maintained in RMPI-1640 supplemented with 10% FBS, 1% L-glutamine, 1% Antibiotic-Antimycotic (Gibco, Waltham, Mass), and 100 IU/mL recombinant human IL-2 (provided by Craig W. Reynolds, Frederick Cancer Research and Development Center, National Cancer Institute, National Institutes of Health, Frederick, Md). B cells were transformed as described[E9] and maintained in RMPI-1640 supplemented with 20% FBS, 1% L-glutamine, and 1% Antibiotic-Antimycotic (Gibco).

Intracellular flow cytometry

Cells were fixed with 2% paraformaldehyde and permeabilized with 0.5% saponin, or using commercial kits (Cytofix/Cytoperm, 554722 from BD Biosciences; Foxp3/Transcription Factor Fixation/Permeabilization Concentrate and Diluent, 00-5521-00 from eBioscience). Primary and secondary antibody dilutions and washings were performed in saponin-containing buffer. Intracellular C3 detection was performed by flow cytometry using several mouse anti-human C3-specific mAbs (Fig E4): SIM320.12.2.1 (iC3b/C3dg[1]) and SIM320.12.3.1 (iC3b/C3dg[2]) were produced in-house and detect a fI-cleavage–dependent neoepitope of the C-terminal domain of both iC3b and C3dg fragments (IgG_1 isotype); clone 2991 (ab11873 from Abcam, Cambridge, United Kingdom, IgG_1 isotype) detects a C3 convertase–dependent C3a neoepitope. CD46 (555948 from BD Biosciences) or CD19 (A07771, PE-Cy5 from Beckman Coulter, Brea, Calif) were used as positive controls for T- or B-cell lines, respectively. For purified mAb, several phycoerythrin-conjugated goat anti-mouse IgG secondary antibodies were used: goat F(ab′)2 anti-mouse IgG (H+L) (731856 from Beckman Coulter or 12-4010-87 from eBioscience) and goat anti-mouse IgG (550589, BD Biosciences).

ELISA and Western blot

Ninety-six–well plates were coated with a rabbit anti-human C3 antibody (produced in-house) in PBS at 4°C. After blockage with Tris-Tween 1% BSA for 1 hour at room temperature (RT), serial dilutions in Tris-Tween 1% BSA of plasma samples were added and incubated for 1 hour at RT. C3 was detected using a mouse anti-human C3 mAb (produced in-house, clone SIM27) for 1 hour at RT followed by a peroxidase-labeled goat anti-mouse incubation for 30 minutes at RT. For detection we used OPD (o-phenylenediamine dihydrochloride) substrate. The reaction was stopped with 10% sulfuric acid. Absorbance was measured at 492 nm. Purified human C3 was used for the calibration curve. All samples were tested in duplicate.

Human C3 was detected by Western blot after SDS-PAGE of plasma samples under reducing conditions using a polyclonal rabbit anti-human C3 antibody (produced in-house).

Confocal microscopy

For subcellular localization analysis of C3a and iC3b/C3dg fragments, cells were fixed and permeabilized using Foxp3/Transcription Factor Fixation/Permeabilization Concentrate and Diluent (00-5521-00 from eBioscience), and blocked with 1× Permeabilization Buffer (00-8333-56 from eBioscience) with 1% hIgG + 10% FBS (Gibco). Primary and secondary antibody dilutions and staining washes were also performed in 1× Permeabilization Buffer. C3a and iC3b/C3dg fragments were detected using the same mAb as for intracellular flow cytometry (Fig 2, *B*). Subcellular compartments were detected using rabbit anti-human polyclonal antibodies (from Thermo-Fisher Scientific, Waltham, Mass): GM130 (Cis-Golgi, PA1-077), Trans-Golgi Network 46 (Trans-Golgi, PA1-1069), EEA1 (Early endosome, PA1-063A), and Lamp1 (Lysosome, PA1-654A). Alexa Fluor 488-conjugated goat anti-Mouse IgG (H+L) Superclonal and Alexa Fluor 555-conjugated goat anti-Rabbit IgG (H+L) Superclonal were used as secondary antibodies (A28175 and A27039, from Invitrogen, Waltham, Mass). Mouse IgG_1 (eBisocience) and rabbit IgG (Abcam) were used as isotype controls. Cells were mounted using ProLong Gold with 4′-6-diamidino-2-phenylindole, dihydrochloride (P36935 from Molecular Probes, Eugene, Ore) and images (represented as maximum intensity projections from Z-stacks) were obtained in the Center for Cytometry and Fluorescence Microscopy of Complutense University with an Olympus FV1200 Confocal Microscope and analyzed with Fiji/ImageJ (National Institutes of Health). Pearson correlation coefficients *Rcoloc* from Fiji/ImageJ were used for statistical analysis, and colocalization was accepted when r was more than 0.5 (dashed lines in Fig 2, *C*).

For intracellular C3a expression analysis after TCR activation, cells were analyzed before or after activation in 48-well plates coated with 2.0 μg/mL mAb against CD3 (OKT3 clone, purified from a hybridoma in Kemper's Lab), for 36 hours. Cells were fixed and permeabilized using Cytofix/Cytoperm (554722 from BD Biosciences), and blocked with 1× Perm/Wash (554723 from BD Biosciences) with 10% FBS (Gibco). Primary and secondary antibody dilutions and staining washes were also performed in 1× Perm/Wash buffer. C3a and iC3b/C3dg fragments were detected using the same mAb as for intracellular flow cytometry (above and Fig E5); Alexa Fluor 488-conjugated rabbit anti-mouse IgG (H+L) from Invitrogen (A11059) was used as secondary antibody. Cells were mounted with VECTASHIELD HardSet Antifade Mounting Medium with 4′-6-diamidino-2-phenylindole, dihydrochloride (H-1500, from Vector Laboratories, Inc) and images (represented as maximum intensity projections from Z-stacks) were obtained in the King's College London Nikon Imaging Centre by confocal microscopy with an A1R Si Confocal Microscope (×100 objective) and analyzed with NIS Elements software (Nikon, Surrey, UK).

Statistical analysis

Results are shown either as scatter dot plots compared with the normal 5th, 50th, and 95 percentiles in boxes, or as mean + or ± SD. Two-tailed Student t test, 1-way ANOVA with Tukey multiple comparison post hoc test, and Pearson correlation coefficient method with 2-tailed P value were performed in the latter using GraphPad Prism (La Jolla, Caif), and significance was considered only when P values were less than .05 ($*P < .05$; $**P < .01$; $***P < .001$).

DISCUSSION

Clinical relevance

The memory B-cell development impairment shown in both primary and secondary C3-deficient patients (Fig 1) did not cause an equivalent functional impairment *in vitro* (Fig E3) or *in vivo* (Table E2), and it did not correlate with the severity of the kidney disease (Table E3). Correspondingly, despite reports of recurrent bacterial infections in some primary plasma C3–deficient patients,[1,4,E10] our cohort, as well as other's,[5] did not show clinical features suggestive of severe B-cell defects, such as bacterial, sinopulmonary infections, or gastrointestinal infections by *Giardia lamblia* or rotavirus. Other examples of impaired B-cell transit from naive to memory stages with normal levels of specific antibodies have been reported, for instance, in human CD21/CR2 (the C3 fragment receptor) deficiency.[E11] In contrast, human deficiencies of other components of the B-cell coreceptor, such as CD19 or CD81, are associated with both impaired memory B-cell development and defective antibody responses,[E12-E14] suggesting discrete roles for each coreceptor chain in B-cell differentiation (see graphical abstract in Fig E6). European vaccination guidelines were used in our cohort, which was carefully followed-up by top-notch specialists. This may explain the absence of overt clinical correlates of B-cell dysfunction, which may be clinically more relevant for the management of complement deficiency patients in countries where health conditions or vaccinations are below Western standards.

It could be argued that some compensatory mechanism could partly replace the lack of plasma C3 in patients to provide signals that support normal T- and B- lymphocyte responses. However, we find such compensation unlikely because C3 deficiency affects all

complement activation pathways (classical, lectin, and alternative) because C3 activation is the central step where all converge. Indeed, the alternative complement activation pathway supports up to 80% of all complement activation,[E15] and immunoglobulin deposits, as found in most patients in our cohort (Henoch-Schönlein purpura, membranoproliferative glomerulonephritis, Table E3), indicate a defect in immune complex clearance, which depends on the classical complement pathway.

Impact of C3 mutations

We report immunological features of patients carrying LOF *C3* mutations causing primary C3 deficiency (p.T56TfsX16 and p.G561D), and GOF *C3* mutations and LOF *CFI* mutations causing secondary C3 deficiency (p.W552C and p.R1042G[E16] for *C3*, and p.C247G[E2] and p.A258T[E2] for *CFI*, Fig E4, *B*, and Table E1), which were leaky in all cases (Fig 2, *A*, right), perhaps explaining intracellular C3 detection. LOF *C3* mutations reduce plasma C3 levels by generating misfolded proteins, likely degraded. GOF *C3*-dominant mutations[4,E16] reduce plasma C3 levels by generating abnormal alternative pathway C3 convertases (C3bBb), which cannot be inactivated and thus consume the C3 encoded by the normal allele. LOF *CFI* mutations reduce C3 levels by preventing C3b degradation, allowing C3bBb to consume normal C3. A graphical abstract summarizes these mechanisms (Fig E7).

The LOF *C3* mutations resulted in distinct biochemical features (Fig 2, *A*, right): the frameshift p.T56TfsX16 mutation is very severe but allowed for minute amounts of a slightly larger α C3 protein (normal size is 110 kDa), whereas the missense p.G561D mutation seemed less severe and its normal-sized product was cleaved into C3b (101 kDa α' chain). However, in all cases, intracellular C3 fragments were detected (Fig 2 and Fig E5), although slightly less in primary C3-deficient T, but not B, cells (Fig 2, *A*). In addition, C3 fragments accumulated in degradation compartments, which could impair C3 exocytosis (Fig 2, *C*, right, and graphical abstract in Fig E8). These data strongly support our previous contention that complete (combined intracellular and extracellular) C3 (or C5) deficiency may not exist in humans.[8]

Taken together, our data indicate an essential role for plasma C3 in the development of memory B, but not T, lymphocytes, and support disparate regulation of plasma C3 and intracellular C3 content in lymphocytes.

REFERENCES

E1. Martinez-Barricarte R, Heurich M, Valdes-Canedo F, Vazquez-Martul E, Torreira E, Montes T, et al. Human C3 mutation reveals a mechanism of dense deposit disease pathogenesis and provides insights into complement activation and regulation. J Clin Invest 2010;120:3702-12.
E2. Ponce-Castro IM, González-Rubio C, Delgado-Cerviño EM, Abarrategui-Garrido C, Fontán G, Sánchez-Corral P, et al. Molecular characterization of Complement Factor I deficiency in two Spanish families. Mol Immunol 2008;45:2764-71.
E3. González-Rubio C, Ferreira-Cerdán A, Ponce IM, Arpa J, Fontán G, López-Trascasa M. Complement factor I deficiency associated with recurrent meningitis coinciding with menstruation. Arch Neurol 2001;58:1923-8.
E4. Tangye SG, Pillay B, Randall KL, Avery DT, Phan TG, Gray P, et al. Dedicator of cytokinesis 8-deficient CD4+ T cells are biased to a TH2 effector fate at the expense of TH1 and TH17 cells. J Allergy Clin Immunol 2017;139:933-49.
E5. Randall KL, Chan SS, Ma CS, Fung I, Mei Y, Yabas M, et al. DOCK8 deficiency impairs CD8 T cell survival and function in humans and mice. J Exp Med 2011;208:2305-20.
E6. Roederer M. Interpretation of cellular proliferation data: avoid the panglossian. Cytometry A 2011;79:95-101.
E7. Pantazis P, Kalyanaraman VS, Bing DH. Synthesis of the third component of complement (C3) by lectin-activated and HTLV-infected human T-cells. Mol Immunol 1990;27:283-9.
E8. Yssel H, de Waal Malefyt R, Duc Dodon MD, Blanchard D, Gazzolo L, de Vries JE, et al. Human T cell leukemia/lymphoma virus type I infection of a CD4+ proliferative/cytotoxic T cell clone progresses in at least two distinct phases based on changes in function and phenotype of the infected cells. J Immunol 1989;142:2279-89.
E9. Tosato G, Cohen JI. Generation of Epstein-Barr virus (EBV)-immortalized B cell lines. Curr Protoc Immunol 2007 Chapter 7:Unit 7 22.
E10. da Silva KR, Fraga TR, Lucatelli JF, Grumach AS, Isaac L. Skipping of exon 27 in C3 gene compromises TED domain and results in complete human C3 deficiency. Immunobiology 2016;221:641-9.
E11. Thiel J, Kimmig L, Salzer U, Grudzien M, Lebrecht D, Hagena T, et al. Genetic CD21 deficiency is associated with hypogammaglobulinemia. J Allergy Clin Immunol 2012;129:801-10.e6.
E12. van Zelm MC, Reisli I, van der Burg M, Castano D, van Noesel CJ, van Tol MJ, et al. An antibody-deficiency syndrome due to mutations in the CD19 gene. N Engl J Med 2006;354:1901-12.
E13. van Zelm MC, Smet J, Adams B, Mascart F, Schandene L, Janssen F, et al. CD81 gene defect in humans disrupts CD19 complex formation and leads to antibody deficiency. J Clin Invest 2010;120:1265-74.
E14. Vince N, Boutboul D, Mouillot G, Just N, Peralta M, Casanova JL, et al. Defects in the CD19 complex predispose to glomerulonephritis, as well as IgG1 subclass deficiency. J Allergy Clin Immunol 2011;127:538-41, e1-5.
E15. Harboe M, Mollnes TE. The alternative complement pathway revisited. J Cell Mol Med 2008;12:1074-84.
E16. Schramm EC, Roumenina LT, Rybkine T, Chauvet S, Vieira-Martins P, Hue C, et al. Mapping interactions between complement C3 and regulators using mutations in atypical hemolytic uremic syndrome. Blood 2015;125:2359-69.
E17. Elvington M, Liszewski MK, Bertram P, Kulkarni HS, Atkinson JP. A C3(H20) recycling pathway is a component of the intracellular complement system. J Clin Invest 2017;127:970-81.

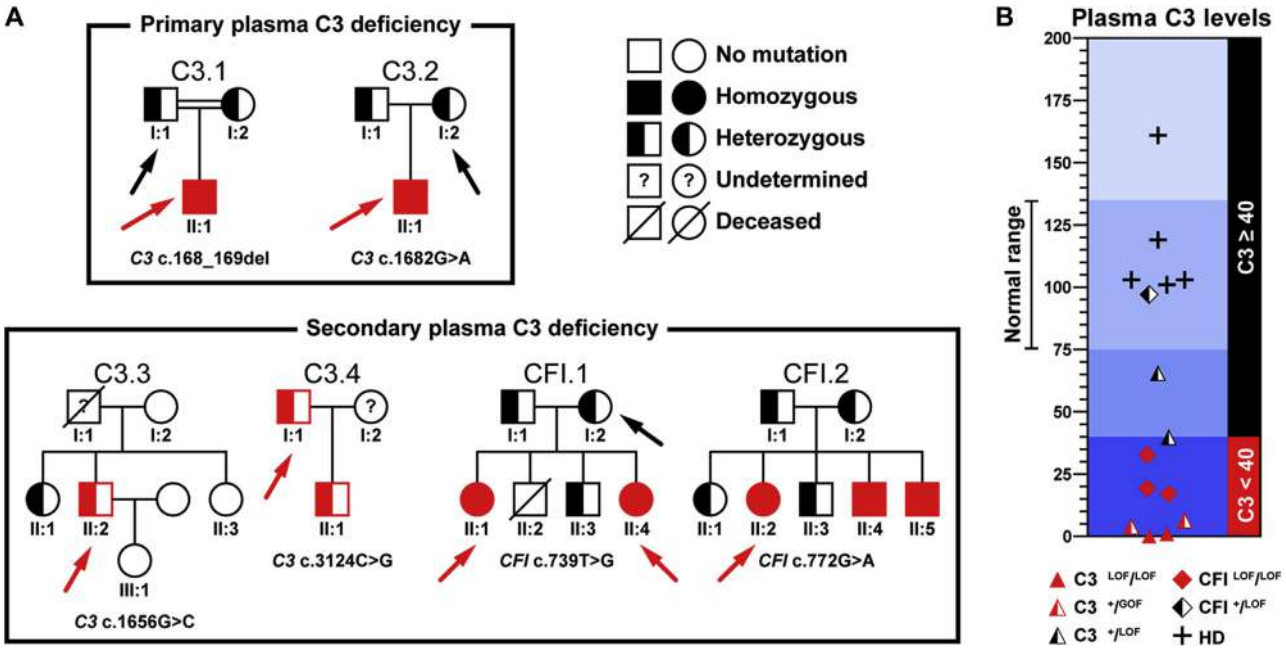

FIG E1. Cohort of studied individuals. **A,** Pedigrees from the 6 families studied; mutations in *C3* or *CFI* are shown below each family tree. *Arrows* indicate studied individuals (red for patients, black for HCs) in each family. **B,** All patients showed plasma C3 levels below 40 mg/dL *(right)*, which was considered a threshold for further analyses.

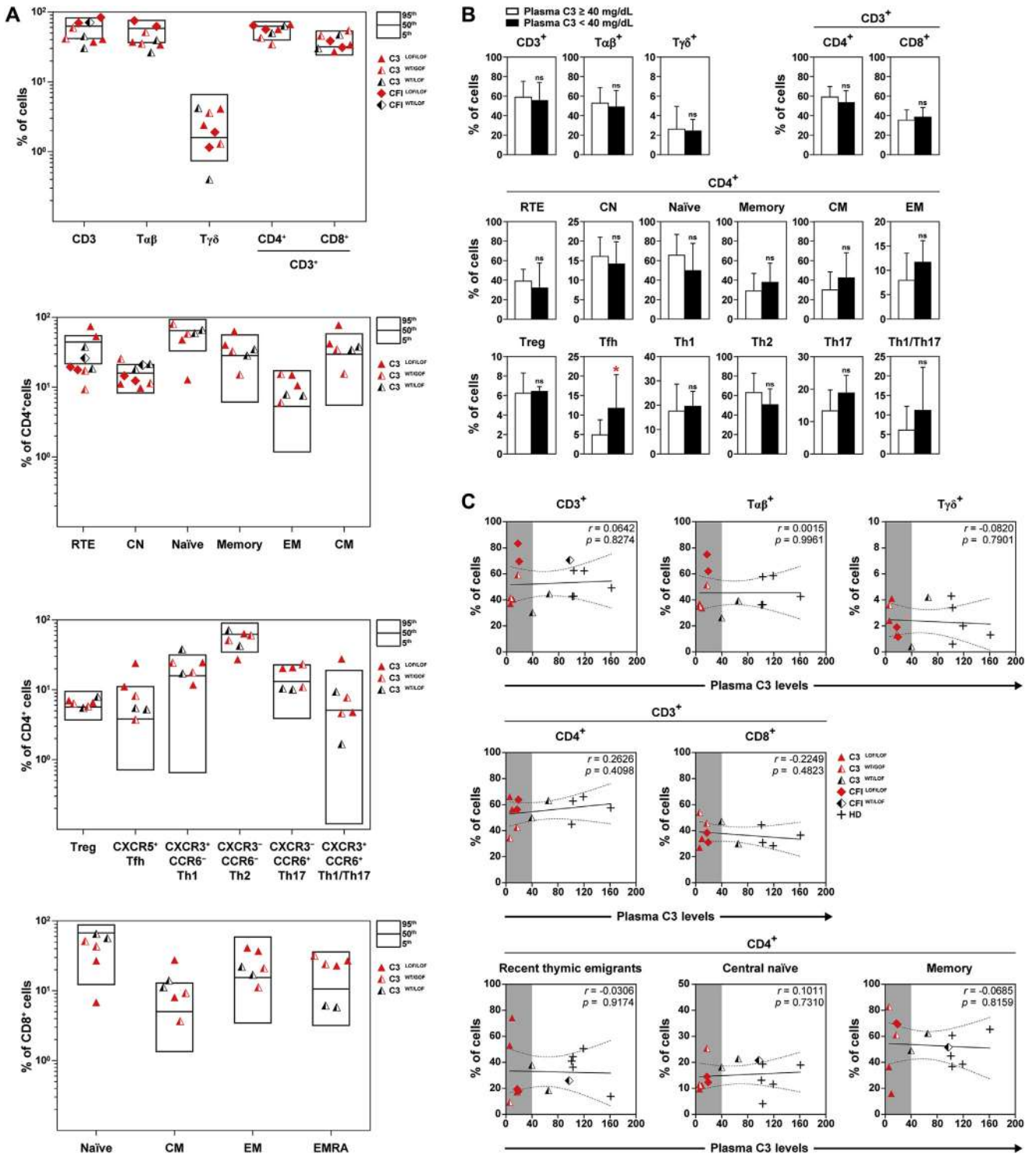

FIG E2. T-lymphocyte immunophenotype analysis. **A,** T-cell subset distribution compared with normal 5th, 50th, and 95th percentiles (boxes; n = 17 HDs). Each symbol represents an individual from a single experiment. **B,** Statistical analysis comparing T-cell subsets (mean + SD) of individuals below (patients) or above (HDs + HCs) the 40 mg/dL plasma C3 threshold. **C,** Correlation between T-cell subsets and plasma C3. *ns*, Nonsignificant; *r*, Pearson correlation coefficient. Solid lines are the best fit after linear regression; dashed lines are their 95% CIs. Gray areas mark the less than 40 mg/dL plasma C3 range. Symbols as in Fig E1, *B*. $*P < .05$.

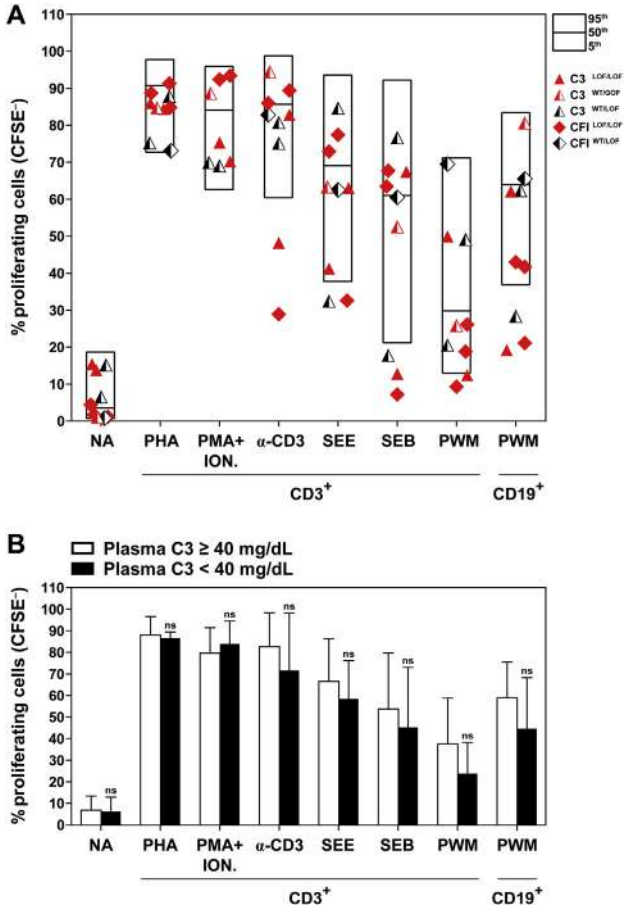

FIG E3. Lymphocyte proliferation in response to different stimuli. **A,** Scatter dot plots of patients and HCs T ($CD3^+$) and B-cell ($CD19^+$) proliferation in response to the indicated stimuli measured as % $CFSE^-$ cells after 5 days compared with normal 5th, 50th, and 95th percentiles (boxes; n = 18 HDs). **B,** Statistical analysis comparing lymphocyte responses (mean + SD) of individuals below (patients) or above (HDs + HCs) the 40 mg/dL plasma C3 threshold. *CFSE*, Carboxyfluorescein succinimidyl ester; *NA*, nonactivated; *ns*, nonsignificant; *PWM*, pokeweed mitogen; *SEE*, *Staphylococcal* Enterotoxin E; *SEB*, *Staphylococcal* Enterotoxin B.

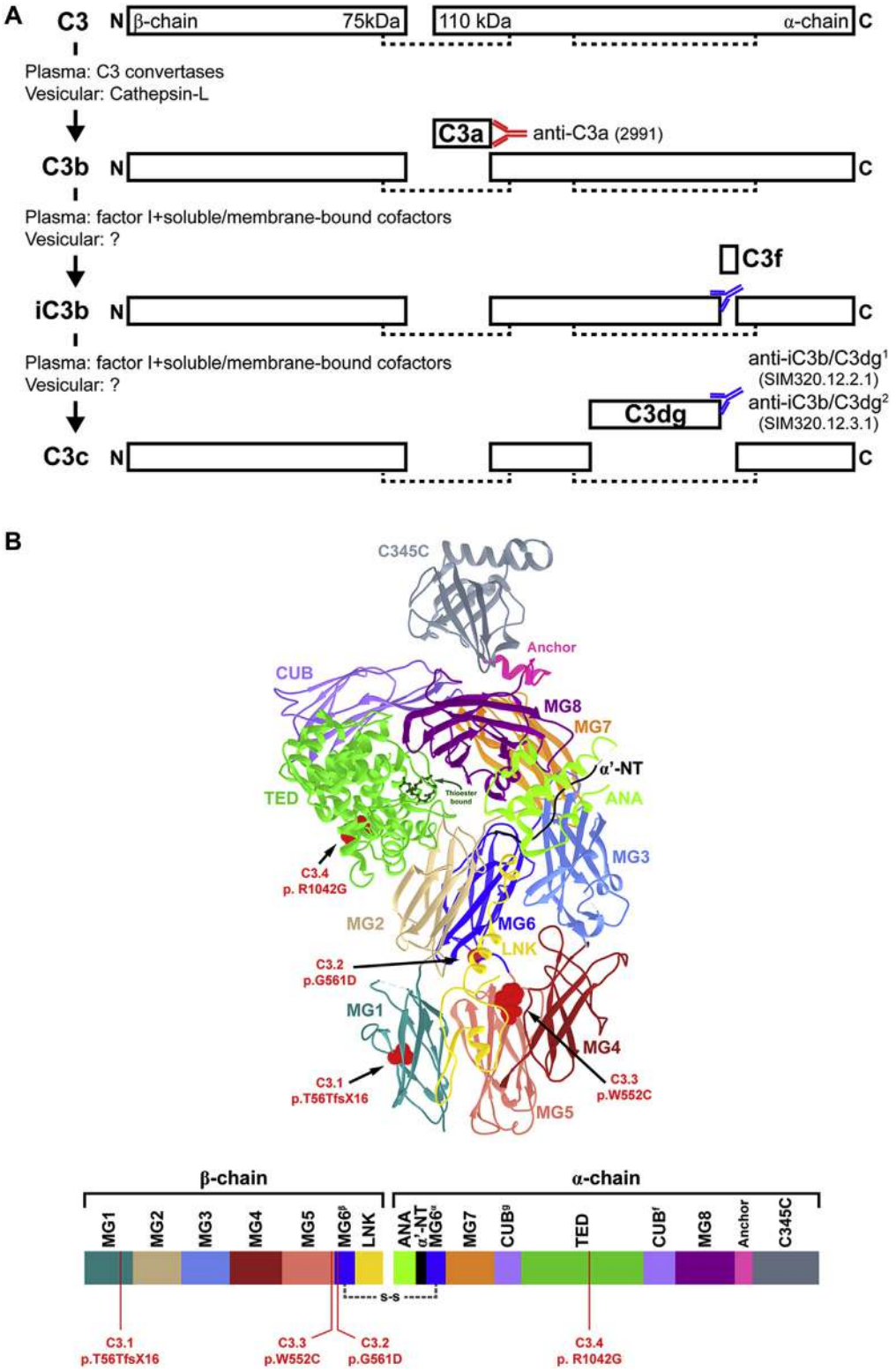

FIG E4. A, Diagram of native C3 (top) and its fragments and plasma or vesicular enzymes involved, including the binding sites in C3a, iC3b, and C3dg of the indicated mAb (clones between parentheses). **B,** The mutations in plasma C3–deficient patients from Table E1 are shown in native C3.

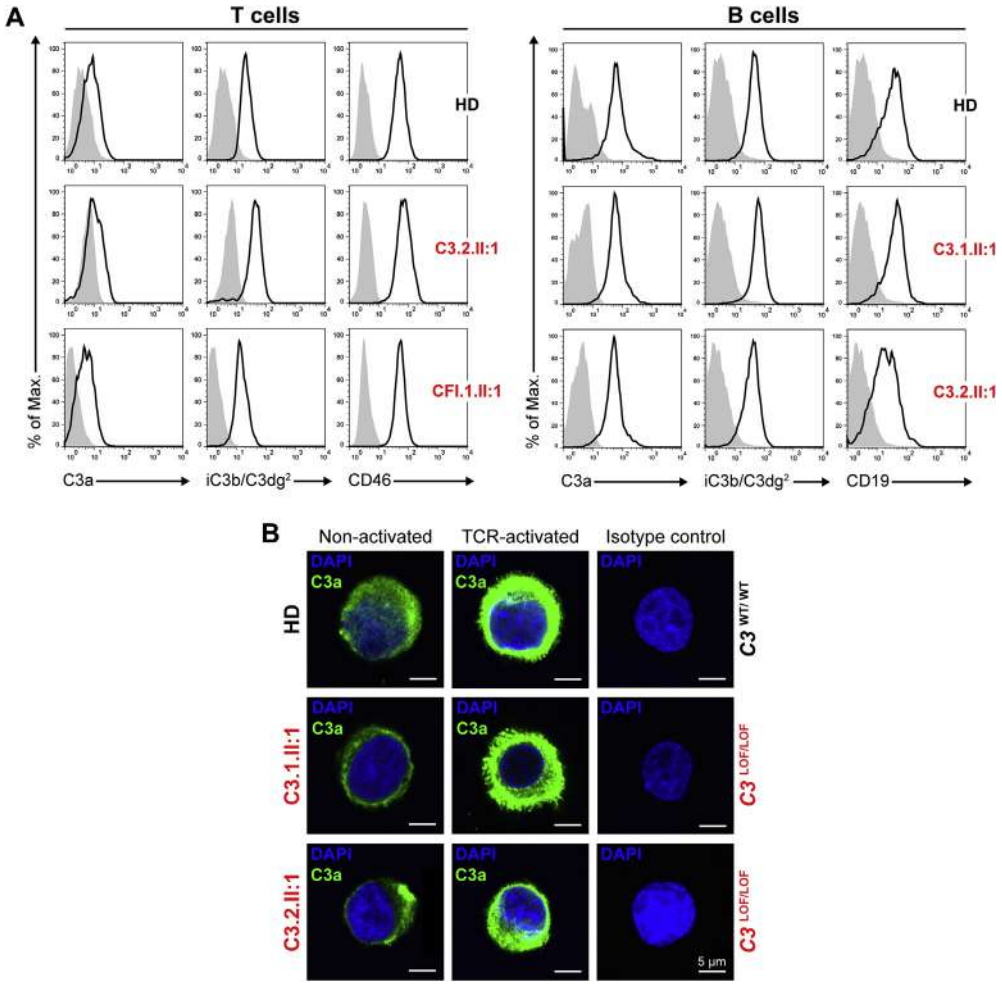

FIG E5. Intracellular C3 analysis in T-cell lines from plasma C3–deficient patients. **A,** Representative intracellular C3a, iC3b/C3dg, and CD46 or CD19 expression in T (left) and B (right) lymphoblastoid cell lines derived from the indicated primary or secondary plasma C3–deficient patients compared with isotype controls (gray histograms). **B,** Intracellular C3a expression using mAb 2991 in T-cell lines from primary plasma C3–deficient patients (C3.1.II:1 and C3.2.II:1) and an HD, after TCR activation for 36 hours, measured by confocal microscopy (magnification ×100).

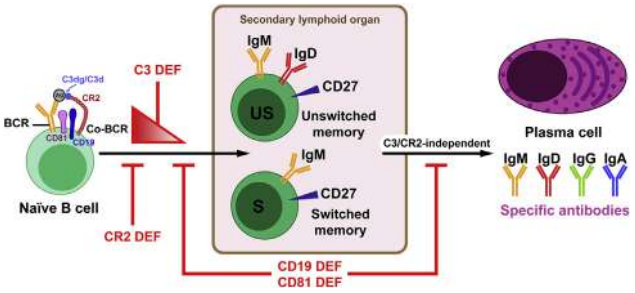

FIG E6. Differential effects of primary deficiencies of B-cell coreceptor components or ligands in B-cell differentiation and antibody synthesis. *BCR*, B-cell receptor; *DEF*, deficiency.

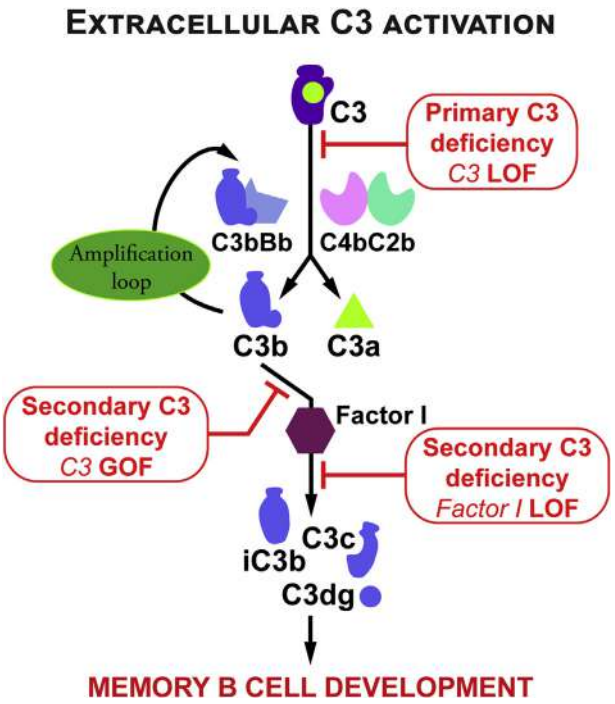

FIG E7. Impact of primary and secondary plasma C3 deficiencies due to LOF/GOF *C3* and LOF *CFI* mutations in extracellular C3 activation.

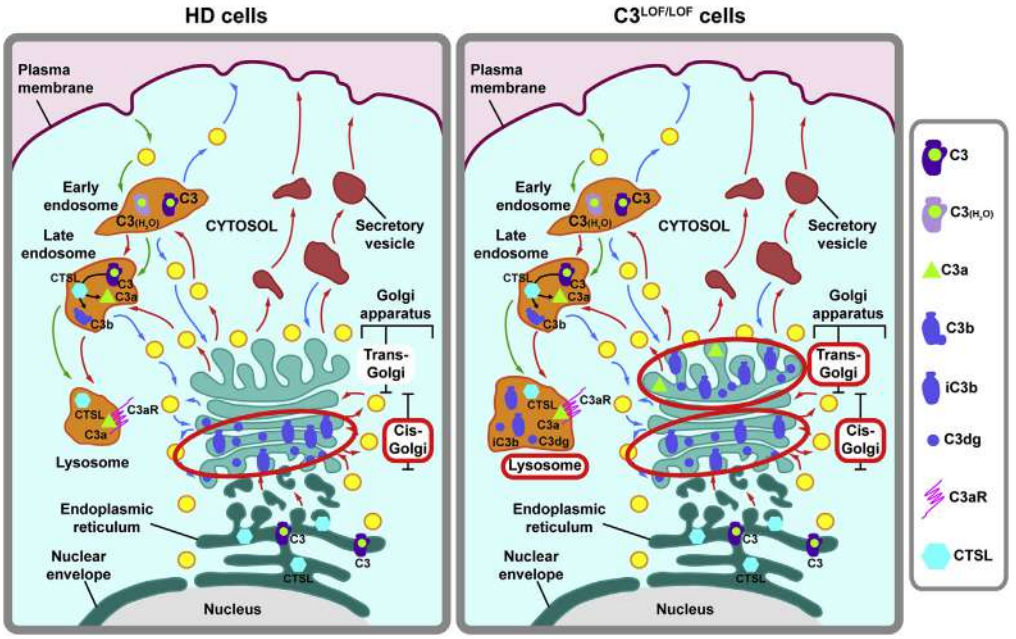

FIG E8. Subcellular accumulation of C3 fragments in vesicular traffic degradation compartments of primary C3–deficient T cells *(right)* compared with HD T cells *(left)*, combining our results and previous data.[6,E17] Red arrows identify biosynthetic-secretory pathways; *blue arrows* denote retrieval/recycling pathways; *green arrows* identify endocytic pathways. *C3aR*, C3a receptor; *CTSL*, cathepsin-L.

TABLE E1. Genetic data and plasma C3 and serum fI levels

Family			Mutation						Plasma C3 (mg/dL)*		
							Type				
Code	ID	Plasma C3 deficiency	Gene	Exon	Nucleotide	Amino acid	a‡	b§	≥40	<40¶	fI (%)
C3.1	I:1	HC	*C3*	2	c.168_169del	p.T56TfsX16	FS	$C3^{WT/LOF}$	**65**		ND
	II:1	Primary						$C3^{LOF/LOF}$		**<6**	76.2
C3.2	I:2	HC	*C3*	13	c.1682G>A	p.G561D	MS	$C3^{WT/LOF}$	**40**		ND
	II:1	Primary						$C3^{LOF/LOF}$		**9**	88.0
C3.3	**II:2**	Secondary	*C3*	13	c.1656G>C	p.W552C	MS	$C3^{WT/GOF}$		**17**	ND
C3.4†	**I:1**	Secondary	*C3*	24	c.3124C>G	p. R1042G	MS	$C3^{WT/GOF}$		**<6**	ND
CFI.1†	I:2	HC	*CFI*	5	c.739T>G	p.C247G	MS	$CFI^{WT/LOF}$	97		ND
	II:1	Secondary						$CFI^{LOF/LOF}$		**19**	**0.1**
	II:4	Secondary						$CFI^{LOF/LOF}$		**17**	**0.0**
CFI.2†	**II:2**	Secondary	*CFI*	5	c.772G>A	p.A258T	MS/Sp	$CFI^{LOF/LOF}$		**33**	**2.4**

Normal local ranges for plasma C3 or serum fI are 75-135 mg/dL or 77%-115% of normal human serum, respectively; values in bold are below normal range. Subject identification (ID) as in Fig E1, patients in boldface.

ND, Not determined.

*Mean values of 2-6 determinations (nephelometry).

†Reported previously.[E2,E16]

‡By effect on structure: FS, frameshift; MS, missense; Sp, splicing.

§By effect on protein function: WT, wild type; LOF, loss-of-function; GOF, gain-of-function.

¶All with clinical symptoms.

TABLE E2. Serum immunoglobulins and vaccine-specific antibodies

Family			Immunoglobulins			Bacteria			Virus		
Code	ID	Age*	IgG	IgA	IgM	Strep. pneumoniae	Tetatuns toxoid	Diphtheria toxoid	Rubella	Varicella	Measles
C3.1	I:1	45	1280	172	83	14.0	16.2	0.1	−	+	+
	II:1	13	845	203	97	4.7	26.3	1.3	−	+	+
C3.2	I:2	40	963	215	224	24.7	6.9	0.4	+	+	+
	II:1	8	1630	315	116	88.0	8.5	0.5	+	+	+
C3.3	**II:2**	35	746	230	64	ND	ND	ND	ND	ND	ND
CFI.1	I:2	55	955	262	217	3.6	13.9	0.3	+	+	+
	II:1	36	1130	121	233	5.4	30.1	0.2	+	+	+
	II:4	26	852	226	111	11.7	30.4	0.9	+	+	+
CFI.2	**II:2**	50	1050	333	110	6.5	3.1	0.03	+	+	+
Normal range			725-1900 mg/dL	50-340 mg/dL	45-280 mg/dL	>0.1 μg/mL	>2.4 μg/mL	>0.01 IU/mL	+	+	+

Identification (ID) as in Fig E1 (patients in boldface).
−, Negative; +, positive; *ND*, not determined.
*At date of analysis.

TABLE E3. Clinical and immunological features of plasma C3–deficient patients

Code	Plasma C3 deficiency	Age (y)		Main renal pathology	Renal dysfunction stage‡	Other pathologies	Infections§	Current condition	% Memory B cells‖	
		AD*	PA†						Unswitched	Switched
C3.1.II:1	Primary	9	18	MPGN I	1	HSP Arthralgia	Pneumonia (×2)	Normal renal function Mild proteinuria	**2.40**	**1.70**
C3.2.II:1	Primary	1	13	MPGN I	1	HSP Hemolytic anemia Chronic hemolysis Splenomegaly	Streptoccocal pharingytis Viral meningitis, B19 parvovirus	Normal renal function Chronic hemolysis Splenomegaly	8.70	**6.50**
C3.3.II:2	Secondary	23	40	C3G	3	HSP Hypertension Hypercholesterolemia	Septicemia Pneumonia	Proteinuria Mild hematuria	**8.40**	**7.90**
C3.4.I:1	Secondary	45	49	—	1	—	—	Asymptomatic	**6.54**	22.40
CFI.1.II.1	Secondary	23	39	—	—	—	Meningococcal septicemia Meningococcal meningitis	Asymptomatic	**4.20**	**3.90**
CFI.1.II.4	Secondary	14	30	—	—	—	Meningitis	Asymptomatic	**3.70**	**4.70**
CFI.2.II:2	Secondary	19	53	—	—	HSP Chronic juvenile arthritis	Meningococcal meningitis Pneumococcal pneumonia	Asymptomatic	**5.67**	12.88

C3G, C3 glomerulopathy.
*At diagnosis.
†Present age.
‡CKD (chronic kidney disease) stage: minimum 1 to maximum 5. No correlation was found with memory B-cell levels, not shown.
§Bacterial, viral, other; number of infections is marked between parentheses.
‖Normal ranges (5th-95th percentiles) for memory B cells: 8.6% to 28.4% unswitched and 11.4%-32.6% switched. Boldface means out of range.